FE CALCULATIONS OF *J*-INTEGRAL IN A CONSTRAINED ELASTOMERIC DISC WITH CRACK SURFACE PRESSURES AND ISOTHERMAL LOADS

H. K. Ching
Materials Technology Center
Southern Illinois University
Carbonale, IL 62901, U. S. A

C. T. Liu
AFRL/PRSM
10 E. Saturn Blvd.
Edwards AFB, CA 93524, U. S. A.

S. C. Yen
Materials Technology Center
Southern Illinois University
Carbonale, IL 62901, U. S. A.

ABSTRACT

In this study, we performed linear and nonlinear FE (Finite Element) analyses to compute *J*-integrals for a centrally perforated star-shaped disc, which was made of an elastomeric material, under crack surface pressures and isothermal loads. Deformations of the disc were constrained by a circular steel ring enclosing the disc. Different crack sizes were assumed to exist in the front of the star-shaped notches. For the linear analysis, material compressibility was modeled with Poisson's varying form 0.48 to 0.4999. In addition, with the presence of the crack surface pressure, the *J*-integral was modified by including an additional line integral. Numerical studies show that the value of the *J*-integral increases with the increase of the crack length, reaches a maximum value at 1in. of crack length, and then decreases gradually. Both linear and nonlinear analyses agree qualitatively but differ quantitatively. It is also found that values of the *J*-integral strongly depend upon the material compressibility.

INTRODUCTION

Defects such as voids and cracks may form in elastomeric materials due to the manufacturing, handling or ageing. To ensure the integrity and reliability for such structural components, fracture toughness should be ascertained so that the onset of the crack growth can be determined based on the fracture resistance of the material. The J-integral is a measure of the fracture toughness, and commonly used as a criterion to determine the maximum operating loads for a given pre-existing defect. Most elastomeric materials such as rubbers and solid propellants exhibit mechanical behavior that remain nonlinearly elastic at large strains and have very little compressibility, and hence these materials are often referred to as fully or nearly incompressible. When these elastomers are loaded in a highly confined state, even a small change in the compressibility can result in dramatic difference of stress distributions. For example, Schapery [1] conducted an experiment for a circular polymeric disk under the hydrostatic tension, and showed that a small change in Poisson's ratio could alter the stress distribution significantly.

Many investigations have been conducted to determine the relationship between the crack-tip stress and strain fields and the energy release rate for rubber-like materials. Thomas [2] was the first to study this relationship experimentally. He found that the average strain energy density in a sheet of rubber was uniquely related to the energy release rate regardless of the specimen type. Thomas's conclusion had been validated later by Andrews [3] and Knauss [4]. Andrews used a microscopic, photoelastic technique to quantify the strain fields around the crack tip whereas Knauss used a printed-grid technique. Morman et al. [5] also gave an analytical solution relating the energy release rate to the crack tip radius.

Rice's development of the *J*-integral [6] gave a mathematical argument to characterize the local stress-strain field around a crack front. The *J*-integral was found to be equivalent to the energy release rate and independent of the path contours. Based on the *J*-integral, several path-independent integrals have been proposed for more general elastic-plastic problems by including non-proportional loading and unloading, thermal strains, and material inhomogeneity. A review about the limitations and salient features of these integrals can be found in Kim and Orange's work [7]. Note that Rice's original form of the *J*-integral is valid even for the nonlinear elastic materials. The problem of a crack in an infinite, thin, and incompressible sheet subjected to a biaxial tension at infinity was studied, within the framework of nonlinear elasticity for a Neo-Hookean material, by Wong and Shield [8], and Chang [9] generalized the *J*-integral for nonlinear elastic materials with finite strains.

1. REPORT DATE **JUN 2004**	2. REPORT TYPE	3. DATES COVERED **-**

4. TITLE AND SUBTITLE	5a. CONTRACT NUMBER
FE Calculations of J-Integrals in a Constrained Elastomeric Disk with Crack Surface Pressure and Isothermal Load	5b. GRANT NUMBER
	5c. PROGRAM ELEMENT NUMBER

6. AUTHOR(S)	5d. PROJECT NUMBER **2302**
H Ching; C Liu; S Yen	5e. TASK NUMBER **0378**
	5f. WORK UNIT NUMBER

7. PERFORMING ORGANIZATION NAME(S) AND ADDRESS(ES) **Air Force Research Laboratory (AFMC),AFRL/PRSM,10 E. Saturn Blvd.,Edwards AFB,CA,93524-7680**	8. PERFORMING ORGANIZATION REPORT NUMBER

9. SPONSORING/MONITORING AGENCY NAME(S) AND ADDRESS(ES)	10. SPONSOR/MONITOR'S ACRONYM(S)
	11. SPONSOR/MONITOR'S REPORT NUMBER(S)

12. DISTRIBUTION/AVAILABILITY STATEMENT
Approved for public release; distribution unlimited

13. SUPPLEMENTARY NOTES

14. ABSTRACT
In this study, we performed linear and nonlinear FE (Finite Element) analyses to compute J-integrals for a centrally perforated star-shaped disc, which was made of an elastomeric material, under crack surface pressures and isothermal loads. Deformations of the disc were constrained by a circular steel ring enclosing the disc. Different crack sizes were assumed to exist in the front of the star-shaped notches. For the linear analysis, material compressibility was modeled with Poisson's varying form 0.48 to 0.4999. In addition, with the presence of the crack surface pressure, the J-integral was modified by including an additional line integral. Numerical studies show that the value of the J-integral increases with the increase of the crack length, reaches a maximum value at 1in. of crack length, and then decreases gradually. Both linear and nonlinear analyses agree qualitatively but differ quantitatively. It is also found that values of the J-integral strongly depend upon the material compressibility.

15. SUBJECT TERMS

16. SECURITY CLASSIFICATION OF:			17. LIMITATION OF ABSTRACT	18. NUMBER OF PAGES **7**	19a. NAME OF RESPONSIBLE PERSON
a. REPORT **unclassified**	b. ABSTRACT **unclassified**	c. THIS PAGE **unclassified**			

The presence of the crack surface tractions, which may be due to ignition pressures or pressurized fluids, is of practical interests in engineering applications. In this regard, the *J*-integral needs to be modified by including an additional line integral so that the path-independence of the *J*-integral can be preserved. Chang and Becker [10] scrutinized the effect of non-conservative surface tractions applied to the crack faces on the energy release rate for a 2D rubber-like material. They pointed out that the usual expression for the energy release rate needed to be modified, and also demonstrated that the energy release rate depended upon the constitutive relation used to model the material response.

In this study, a finite element (FE) analysis was conducted to compute the *J*-integral for a circular elastomeric disc with a pre-existing crack. The disc had a star-shaped hole with six symmetrical notches emanating from the disc's center and was enclosed by a thin steel ring. We assumed that the disk was modeled either as a linearly elastic Hookean material or a nonlinear elastic Ogden material, and the steel ring was modeled as a Hookean material. Material constants obtained from a uniaxial tensile test data were used to describe the Ogden strain energy potential. Three loading conditions, internal pressure, constant thermal load, and combined internal pressure and constant thermal load, were considered. To account for the material compressibility, Poisson's ratio of the Hookean material was assumed to vary from 0.48 to 0.4999.

FORMULATION OF THE PROBLEM

Figure.1 shows a cross-section of the specimen in which an elastomeric disc is enclosed by a thin steel ring. A plane strain state of deformation was assumed to prevail in the body. The star-shaped hole at the center of the specimen had six symmetrically located notches. In order to obtain the *J*-integral as a function of the crack length, a starter crack with 11 different crack sizes, a = 0.05, 0.1, 0.2, 0.4, 0.6, 0.8, 1.0, 2.0, 5.0, 10.0, 15 in, was assumed to exist at the notch tip. The elastomeric disc and the steel casing were modeled as isotropic and homogeneous materials. There loading conditions, international pressure, isothermal load, and combined international pressure and isothermal load, were considered. Deformations of the steel ring were assumed to be infinitesimal and the steel was modeled by Hooke's law with Young's modulus = 29 M*psi*, Poisson's ratio = 0.3, and the coefficient of thermal expansion = $6.5 \times 10^{-6}/^{\circ}$F

We performed the FE analysis using the commercial ABAQUS computer code [11] to calculate the *J*-integral for the problem studied. Due to the symmetry of the specimen geometry and loading conditions, only a 30° sector of the specimen was investigated. Figure 2 exhibits the finite element mesh of the sector for a crack size of 1 in. long, and 4824 8-node quadrilateral elements are used with a dense mesh near the crack tip. Because the elastomeritc material was considered to be fully or nearly incompressible, hybrid elements were adopted in the analysis. Points on the bounding surfaces θ = 0° and θ = 30° were constrained to move radially, and tangential tractions on these surfaces were set equal to zero. The outer surface of the steel ring was taken to be traction free.

The elastomeric disc was assumed to be perfectly bonded to the steel ring so that displacements and surface tractions were continuous across their common interface.

The constitutive behavior of the elastomeric disc was determined by either the Hooke's law for the linear analysis or the Ogden strain energy potential for the nonlinear analysis. The stress-strain curve of the elastomer was obtained by conducting the uniaxial tension test at a constant displacement rate of 200 *in/min*. For the Ogden material with fully incompressibility, the strain energy potential is

$$U = \sum_{i=1}^{N} \frac{2\mu_i}{\alpha_i^2} (\bar{\lambda}_1^{\alpha_i} + \bar{\lambda}_2^{\alpha_i} + \bar{\lambda}_3^{\alpha_i} - 3) \qquad (1)$$

where $\bar{\lambda}_i$ are the deviatoric principal stretches $\bar{\lambda}_i = J^{-\frac{1}{3}}\lambda_i$; λ_i are the principal stretches; and μ_i, α_i are temperature-dependent material parameters. J is the total volume ratio.

The shear modulus μ_0 at zero strain for the Ogden material can be given by

$$\mu_0 = \sum_{i=1}^{N} \mu_i \qquad (2)$$

The elastic volume ratio, J^{el} is related to J by

$$J^{el} = J/(1+\alpha T)^3 \qquad (3)$$

We set N equal to 2 in the Ogden strain energy, and ABAQUS computer code determined the material constants μ_i, α_i from the uniaxial test data through a least-squares-fit procedure. Values of μ_1 and μ_2 determined by ABAQUS are

$$\mu_1 = -160.4 \, psi, \ \mu_2 = 1643 \, psi \qquad (4)$$

Computed values of the axial component of the first Piola-Kirchhoff stress vs. the nominal axial strain are compared with the experimental data in Fig. 3. It is clear that the two sets of data are very close to each other implying that values given in Eq. (4) of μ_1 and μ_2 are very accurate.

For the linear analysis, the elastomer was assumed to obey the Hooke's law with Poisson's ratio ν varying from 0.48 to 0.4999. The stress-strain curve for the Hookean material is also depicted in Fig. 3. The Young's modulus is set equal to the slope of the stress-strain at zero strain and it can be computed by

$$E = 2(1+\nu)\mu_0 \qquad (5)$$

where μ_0 is obtained from Eq. (2).

For both linear and nonlinear analyses, the coefficient of thermal expansion for the disk material equaled $5.6 \times 10^{-6}/^{\circ}$F.

When the inner surface of the hole and the surface of the starter crack, aligned with the $x_1 - \text{axis}$, are loaded by a uniform pressure p, the J-integral for an elastic material is given by

$$J = \int_\Gamma \left(W n_1 - T_{ij} n_j \frac{\partial u_i}{\partial x_1} ds \right) + \int_{\Gamma_c} p \frac{\partial u_2}{\partial x_1} dx_1 \qquad (6)$$

where W is the strain energy density, $\mathbf{u}$ is the displacement of a point, Γ is a closed curve enclosing the crack tip, $\mathbf{n}$ is the outward unit normal to Γ, and T_{ij} is the stress tensor, and Γ_c are the two crack faces. Note that the second term on the right-hand side of (6) represents the work done by the pressure on the crack surfaces. For the thermal load, there is no surface traction on the crack surface and this term makes null contribution to the value of J. For a homogeneous hyperelastic material, T_{ij} equals the first Piola-Kirchhoff stress tensors.

The J-integral can be related to the stress intensity factor K by the Irwin's relation [12]. As the crack is subjected to the pressure load or isothermal load, only mode I deformations exist around the crack. Thus, the J-integral can be written as

$$J = \frac{1 - \nu^2}{E} K_I^2 \qquad (7)$$

RESULTS AND DISCUSSIONS

Figures 4(a) and 4(b) show the dependence of the J-integral on the crack length for the linear and nonlinear analyses under the pressure and thermal loads, respectively. Poisson's ratio in the linear analysis is set equal to 0.4999 in order to compare results with those obtained from the nonlinear analysis. The results of the two analyses agree each other qualitatively but differ quantitatively. In both loading conditions, the J-integral initially increases with an increase in crack length, reaches a maximum value at a crack length of about $1.0 in$, and then gradually decreases with an increase in crack length. The linear analysis gives larger values of the J-integral than those of the nonlinear analysis for each of the crack length.

The differences of the J-integral in the two analyses can be more evident by plotting the maximum principal stress around the crack tip with the crack length of 1in. for the pressure and the isothermal loads. The contours of the in-plane maximum principal stress are exhibited in a small region of 1in.[2] where the crack tip is intensively deformed. As for either the pressure or the isothermal loads, the two sets of the principal stresses look alike but differ a little bit. It is shown that the principal stress induced at a point near the crack tip is compressive for the pressure load while it is tensile for the isothermal load. Note that for the Hookean model a small deformation theory is used whereas for the Ogden model a large deformation theory is used. Thus, the differences in the value of the J-integral are due to not only the material models considered but also the geometrical nonlinearity of the specimen.

To investigate the effect of material compressibility on the computed values of the J-integral, four different Poisson's ratios, $\nu = 0.48, 0.49, 0.499$ and 0.4999, were assumed for the material of the elastomeric disc in the linear analysis. Variations of the J-integral with the crack length are depicted in Figs. 6(a), (b) and (c) for the pressure, isothermal and combined loads, respectively. Although, the results are qualitatively similar to each other for different values of Poisson's ratio, the values of the J-integral vary significantly with the Poisson's ratio under the pressure load. The value of the J-integral for $\nu = 0.48$ reaches as high as 143.3 lb/in, which is approximately 40 times the J-integral value, 3.557 lb/in, for $\nu = 0.4999$. It is clear that a slight difference in material compressibility can drastically change the value of the J-integral for the case of the pressure load, and henceforth for the combined load (Fig. 6(c)). When the disc is subjected to the isothermal load, the values of the J-integral do not vary much as those under the pressure load.

For the crack length of 1 in, we further delineate the variation of J-integral with the Poisson's ratio in Fig. 7. The value of the J-integral decreases sharply with the increase in Poisson's ratio from 0.48 to 0.4999 for the pressure load, while it increases gradually with the increase in Poisson's ratio for the isothermal load. Referring to Eq. (7), the value of J-integral is proportional to K_I, and thus one can verify that the value of J-integral is proportional to p^2 under the pressure load or T^2 under the isothermal load. Therefore, even for the linear analysis, values of the J-integral for the combined load cannot be obtained by adding the energy release rates for the corresponding pressure and isothermal loads. The results of the analyses show that, under pressure load, the increase in ν will decrease the compressibility of the material which, in turn, will decrease the crack opening deformations between the two crack faces (Figure 8(a)). For the thermal load, the deformed shape of the crack faces, plotted in Fig 8(b) for different values of Poisson's ratios, does not differ too much. When the Poisson's ratio is equal to 0.4999, the deformed shapes between the Hookean and Ogden materials are almost indistinguishable. The relationship between the J-integral and the crack opening displacement can be ascertained in Fig. 9 where 2 is defined to be the vertical distance between the opposite ending points on the crack faces. It is found that the value of J-integral is also proportional to ^{2}. For the crack length of 1in, the J-integral can be determined by

$$J = 2.6268 \times 10^3 \delta^2 \qquad (8)$$

Therefore, for the present configuration of the elastomeric disk, the value of the J-integral can be obtained by measuring the crack opening displacement when the disc is loaded.

In classical linear elastic fracture mechanics, the near-tip stress fields can be characterized by a single parameter such as the J-integral or the stress intensity factor. However, previous studies have shown that the T-stress is also an important parameter in describing the state of stresses near the crack tip. For example, Larsson and Carlsson [13] show that the sign and magnitude of the T-stress have a significant effect on the size and shape of a plastic zone around the crack tip. Kirk et al. [14] and Sorem et al. [15] show that the fracture toughness of a

given material can be considerably dependent on the T-stress. It has also been shown by Cotterel and Rice [16] that the T-stress plays an important role in the crack path stability. Figure 10 depicts the variation of T-stress with the crack length for the pressure and isothermal loads when the Poisson's ratio is equal to 0.4999. For both loading cases, the magnitude of the T-stress decreases with the increase of the crack length, and the T-stress is in compression (i.e. negative values of T-stress). Betegon and Hancock [17] have indicated that when the T-stress corresponds to the negative value, crack-tip deformations are dominated by the combination of the J-integral and T-stress. Furthermore, the fracture trajectory is path stable for a cracked specimen with negative T-stress. The dependence of the T-stress on the Poisson's ratio is evinced in Fig. 11. Similar to the J-integral, the value of the T-stress strongly depends on the Poisson's ratio for the pressure load whereas the Poisson's ratio has a negligible effect on the T-stress for the isothermal load. It can be easily verified that T-stress for the combined load can be obtained by adding the values of T-stress from the corresponding pressure and isothermal loads.

CONCLUSIONS

Linear and nonlinear finite element analyses were conducted to obtain the variations of the J-integral with the crack length for an elastomeric disk enclosed by a steel ring. For both analyses, the value of the J-integral increases with an increase in the starter crack length, reaches a maximum value at 1 in. of crack length, and then decreases gradually. The results of the analyses also show that linear analysis leads to a higher value of J-integral than the non-linear analysis. Material compressibility of the disc was also considered by varying the Poisson's ratio from 0.48 to 0.4999 for the Hookean material. For the pressure load, the value of the J-integral strongly depends upon the values of the Poisson's ratio. This is due to the reason that the work done by the crack surface pressure increases noticeably as the value of the Poisson's ratio is decreased, resulting in a significant increase in the J-integral. For the thermal load, the value of J-integral does not differ much with the variation of the Poisson's ratio. It is interesting and important to point out that, even for the linear analysis, the value of J-integral for the combined load cannot be obtained by adding the J-integral values obtained from the pressure and the isothermal loads separately. Dependence of the T-stress on the crack length and material compressibility was also examined. The magnitude of the T-stress decreases with the increase in crack length, and the T-stress is found to be in compression.

ACKOWLEDGEMENTS

REFERENCES

1. Lindsey, G. M., *J. Appl Phys*. 38(12), pp. 4843-4852 (1967).

2. Thomas, A. G., "Rupture of rubber. II. The strain concentration at an inclusion", *J. Polymer Science* 18, 177-188 (1955).

3. Andrew, E. H., "Rupture propagation in hysteresial materials: stress at a notch." *J. Mechanics and Physics of Solids* 11, pp. 231-242 (1963).

4. Knauss, W. G., "Stress near a crack in a rubber sheet", *Experimental Mechanics* 8, pp. 177-181 (1968).

5. Morman, K. N., Mazich, K. A., Oblinger, F. G., Zhang, F., and Killgoar, P. C., "Critical tearing energy in a circumferentially-cracked circular cylinder of rubber under finite deformation", *Int. J. Fracture* 53, pp. 129-157 (1992).

6. Rice J. R., "A path-independent integral and the approximate analysis of strain concentration by notches and cracks", *J. Applied Mechanics* 35, pp. 379-386 (1968).

7. Kim, K. S. and Orange, T. W., "A review of Path-Independent integrals in elastic-plastic fracture mechanics", *American Society for Testing and Materials*, Philadelphia, pp. 713-729 (1988).

8. Wong, F. S., and Shield, R. T., "Large plane deformations of thin elastic sheets of neo-Hookean material", *Z. Angew. Math. Phys*. 20, pp. 176-199 (1969).

9. Chang, S. J., "Path-independent integral for rupture of perfectly elastic materials", *J. Applied Math. and Phys*. 23, pp.149-152 (1972).

10. Chang, J. H., and Becker, E. B., "Finite element calculation of energy release rate for 2-D rubbery material problems with non-conservative crack surface tractions", *Int. J. Num. Math. Eng*. 33, pp. 907-927 (1992).

11. ABAQUS/Standard user's manual 6.2, Hibbitt, Karlsson & Sorensen, Inc., Providence, RI, (2001).

12. Irwin, G. R., "Fracture dynamics. In fracturing of metals", *American Society of Metals*, pp. 147-166 (1948).

13. Larsson, S. G. and Carlsson, A. J. "Influence of non-singular stress terms and specimen geometry on small scale yielding at crack tips in elastic-plastic materials", *J. Mechanics and Physics of Solids*, 21, pp. 263-277 (1973).

14. Kirk, M. T., Koppenhoefer, K. C. and Shih, C. F. "Effect of constraint on specimen dimensions needed to obtain structurally relevant toughness measures", *American Society for Testing and Materials*, Philadelphia, pp. 79-103 (1988).

15. Sorem, W. A., Dodds, R. H. and Rolfe, S. T. "Effects of crack depth on elastic plastic fracture toughness", *Int. J. Fracture* 47, pp. 105-126 (1991).

16. Cotterell, B. and Rice, J. R. "Slightly curved or kinked crack", *Int. J. Fracture* 16, pp. 155-169 (1980).

17. Betegon, C. and Hancock, J. W. "Two-parameter characterization of elastic-plastic crack-tip fields", *J. Applied Mechanics*, 58, pp. 104-110 (1991).
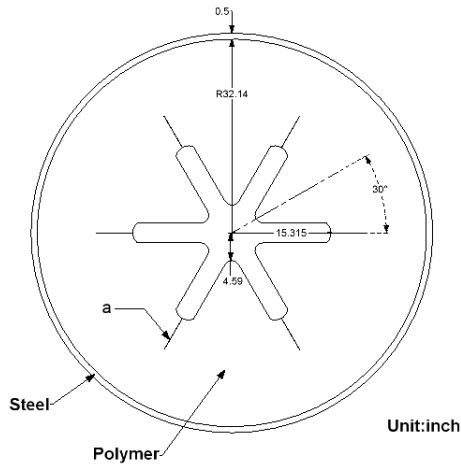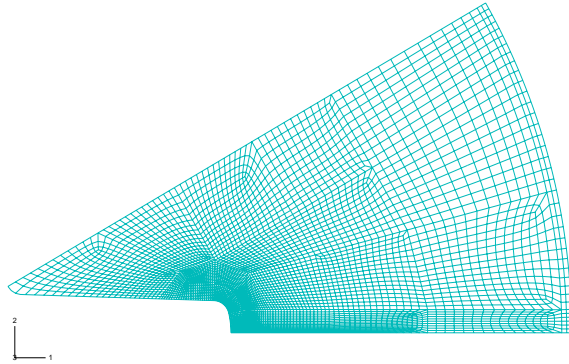
FIGURE 1. Specimen geometry

FIGURE 2. For 1*in* long crack, the finite element mesh with 4824 elements for the analysis of the problem

FIGURE 3. A comparison of the computed and the experimental axial nominal stress vs. nominal strain for the disk material
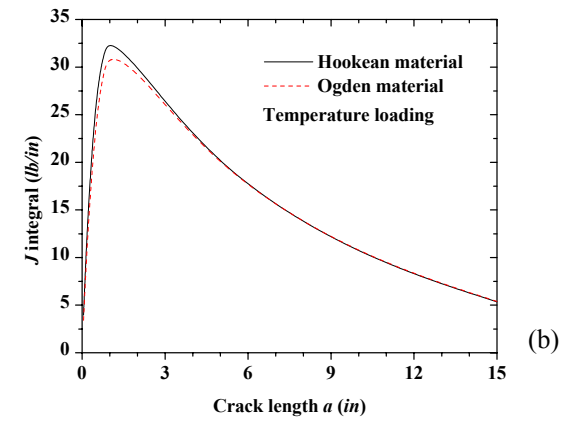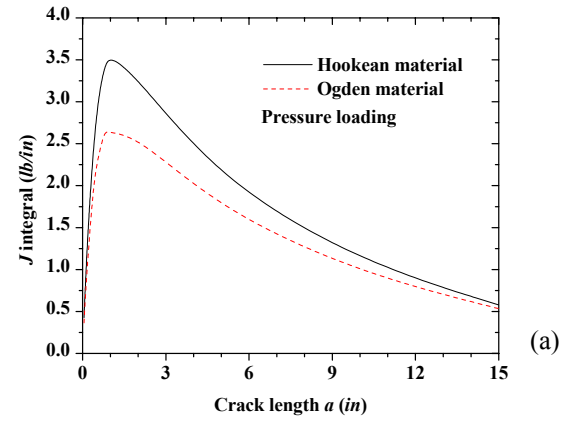

FIGURE 4. Variation of the *J*-integral with the crack length when the disk material is modeled either as a Hookean material or an Ogden material; (a) pressure load (b) isothermal load
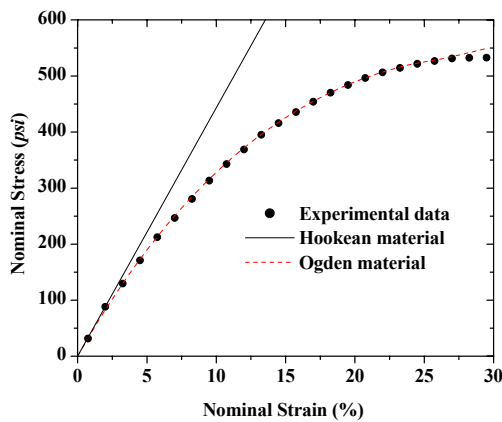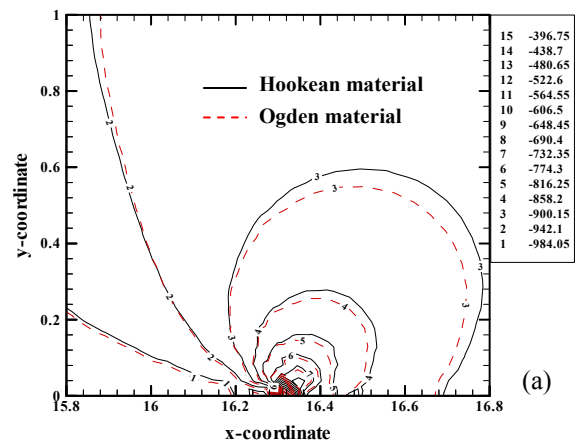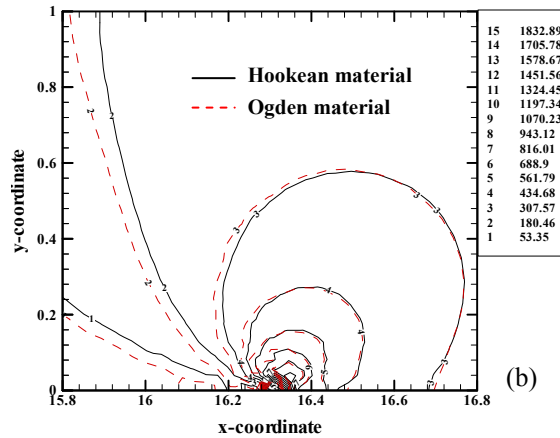
FIGURE 5. Contours of the in-plane maximum principal stress in a small region around the crack tip of 1*in* long crack for Hookean and Ogden materials; (a) pressure load (b) isothermal load
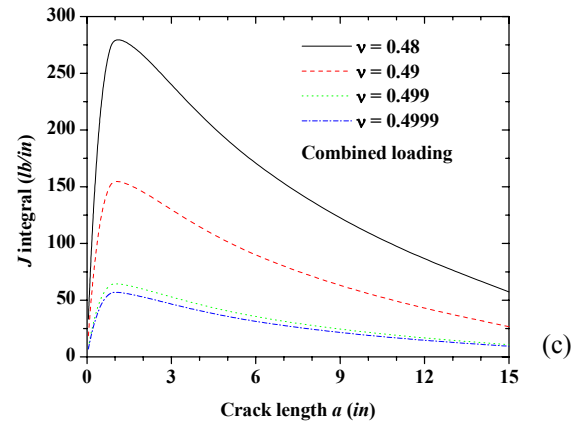
FIGURE 6. Variation of the *J*-integral with the crack length for different values of Poisson's ratio; (a) pressure load (b) isothermal load (c) combined load
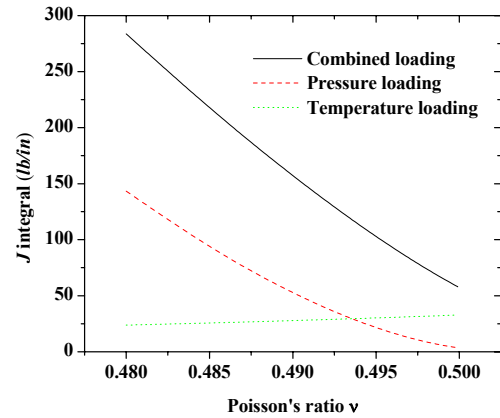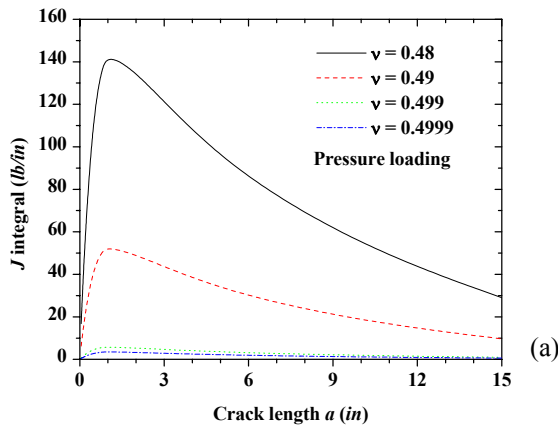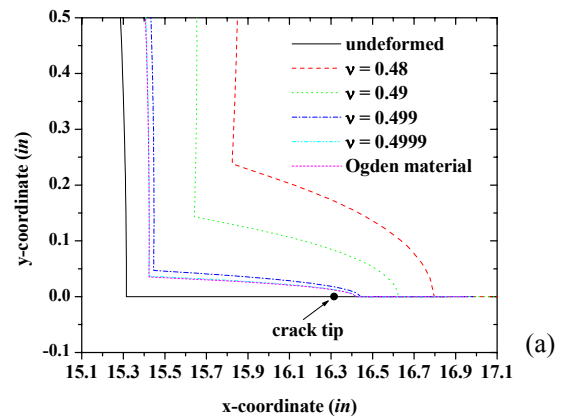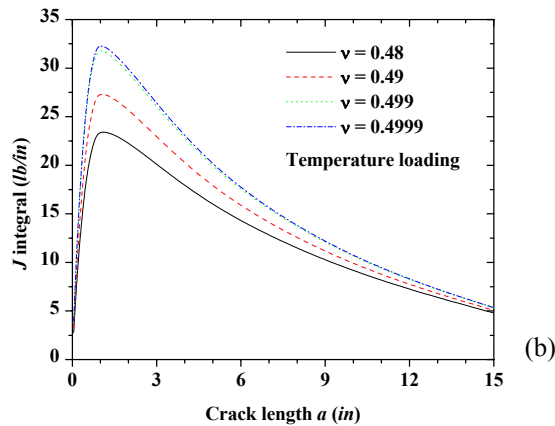

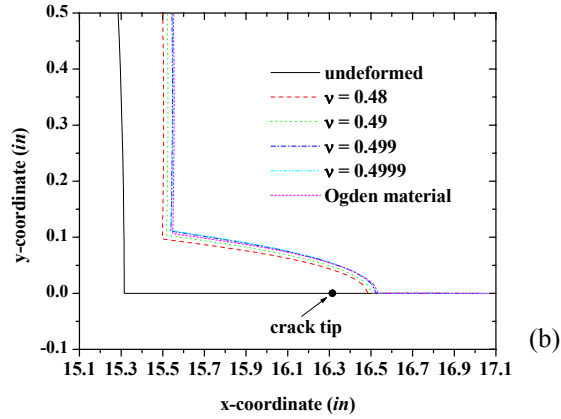**FIGURE 7.** The dependence of the *J*-integral upon Poisson's ratio for three loadings

FIGURE 8. Deformed shapes of the crack face for the Ogden material and Hookean material with different values of Poisson's ratio; (a) pressure load (b) isothermal load
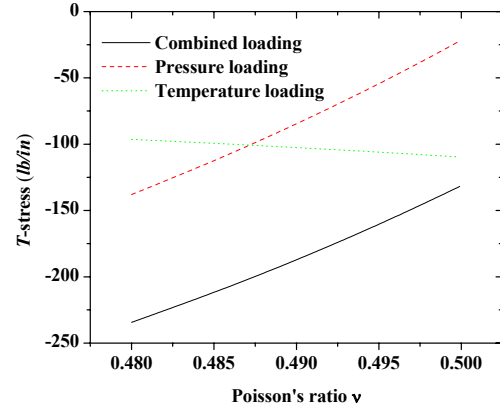

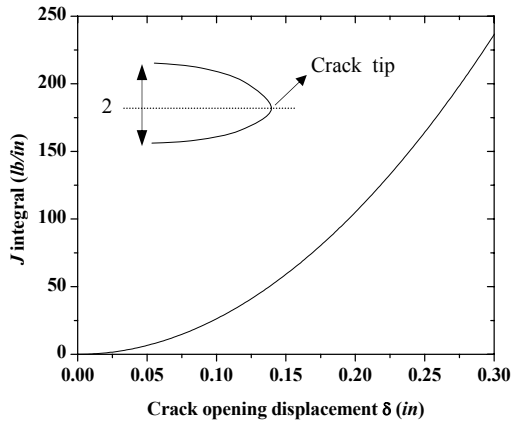**FIGURE 11.** The dependence of the *T*-stress upon Poisson's ratio for three loadings

FIGURE 9. For 1in. long crack, variation of the *J*-integral with the crack opening displacement
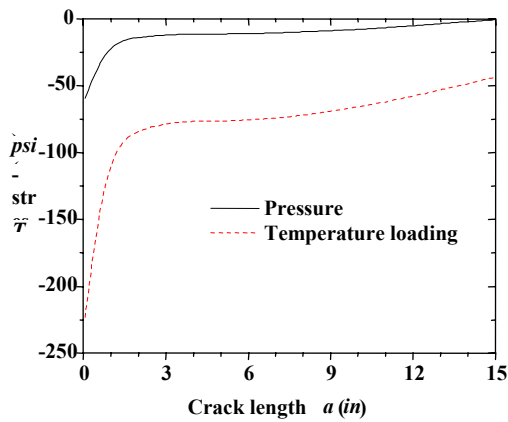

FIGURE 10. Variation of the *T*-stress with the crack length for the pressure and isothermal load